

Physiologic-State-Adaptive Recovery of Aortic Blood Pressure and Flow Using Blind 2-Channel IIR Cardiovascular System Identification

Jin-Oh Hahn, Andrew Reisner, and H. Harry Asada

Abstract— This paper presents the development and analysis of a method to identify a two-channel cardiovascular system using two distinct peripheral blood pressure signals. The method is able to characterize the upper- and lower-limb arterial path dynamics as well as the aortic root impedance, and recover the aortic blood pressure and flow signals fed to it. The blind system identification and input de-convolution algorithms for a class of two-channel infinite impulse response systems are developed and applied to a gray-box model of a two-channel cardiovascular system. Persistent excitation condition, model identifiability and asymptotic variance are analyzed to quantify the method’s validity and reliability. Experimental results based on 83 data segments obtained from a swine subject show that the cardiovascular dynamics can be identified very accurately and reliably, and the aortic blood pressure and flow signals are stably recovered from two distinct peripheral blood pressure signals under diverse physiologic conditions. The benefit of the proposed method is demonstrated by comparing it to a predetermined transfer function describing the cardiovascular dynamics at nominal physiologic conditions.

I. INTRODUCTION

THE physiologic state of the cardiovascular (CV) system can be most accurately assessed by using the aortic blood pressure (BP) and flow (BF). However, standard measurement of these signals entails costly and risky surgical procedures. Thus, most of the practically applicable methods aim to monitor the CV system based on peripheral circulatory signals, e.g. arterial BP at a limb. These include population-based transfer function methods for recovering the aortic BP signal from the upper-limb arterial BP [1], and the estimation of CV parameters from arterial BP measurement [2].

Most of these methods exploit a single peripheral circulatory signal to assess the CV state based on some predetermined model of the CV system. However, it has recently been argued that the state of the CV system cannot be uniquely determined from a single peripheral circulatory signal [3], due to the variability in the vascular geometry, vascular mechanical properties and cardiac ejection. These varying factors are averaged out in the CV parameter estimation methods [2] as well as the group-averaged transfer function methods [1], which use “nominal” parameter values derived from some study population. Care must be taken in applying these, when a subject’s physiologic condition differs sub-

stantially from the group average or the nominal state [4].

In an attempt to extend the CV monitoring techniques to diverse physiologic conditions, this paper presents a method that does not use a predetermined transfer function. Instead, it is identified for each subject under diverse physiologic conditions. In doing so this paper exploits two arterial BP signals observed at two distinct branches in the CV system. Based on the Multi-Channel Blind System Identification theory, both arterial path dynamics are identified, from which the aortic BP and BF signals are recovered adaptively.

The previous works by the author’s group using black-box model structures of the CV system [5]-[6] demonstrated the feasibility of the approach. This paper presents and analyzes a significantly improved algorithm based on a gray-box model structure of the CV system. The validity of the method will be experimentally verified based on 83 data segments obtained from a swine subject. The challenge is to rigorously assess the identifiability of the CV dynamics and quantitatively evaluate the expected error variance. Theoretical analysis addressing the persistent excitation, model identifiability and asymptotic variance will provide a sound basis for evaluating and validating the proposed method, altogether yielding a highly reliable method for characterizing the CV system.

II. THEORETICAL DEVELOPMENT AND ANALYSIS

A. Blind Identification of a Class of 2-Channel IIR Systems

Consider a 2-channel IIR system which creates two distinct output signals $y_1(n)$ and $y_2(n)$ as a result of a common input signal $u(n)$. The dynamics of the channels S_1 and S_2 , $G_1(z)$ and $G_2(z)$, are described as follows, which are assumed to be minimal realizations of S_1 and S_2 :

$$G_i(z) = \frac{\beta_{n_i-r_i}^{(i)} z^{n_i-r_i} + \dots + \beta_0^{(i)}}{z^{n_i} + \alpha_{n_i-1}^{(i)} z^{n_i-1} + \dots + \alpha_0^{(i)}} \triangleq \frac{\beta_i(z)}{\alpha_i(z)}, \quad i=1,2. \quad (1)$$

Since both channels are excited by the common input signal, one of the following correlations between the output signals can be explored to identify the channels S_1 and S_2 , if $G_1(z)$ and $G_2(z)$ possess no common poles and zeros [5], [7]:

$$\begin{aligned} G_1(z)y_2(n) &= G_1(z)[G_2(z)u(n)] \\ &= G_2(z)[G_1(z)u(n)] = G_2(z)y_1(n), \end{aligned} \quad (2a)$$

$$\begin{aligned} G_1^{-1}(z)y_1(n) &= G_1^{-1}(z)[G_1(z)u(n)] \\ &= G_2^{-1}(z)[G_2(z)u(n)] = G_2^{-1}(z)y_2(n). \end{aligned} \quad (2b)$$

Jin-Oh Hahn and H. Harry Asada are with the d’Arbeloff Laboratory for Information Systems and Technology, Massachusetts Institute of Technology (e-mail: stardust@mit.edu, asada@mit.edu).

Andrew Reisner is with the Emergency Department, Massachusetts General Hospital (e-mail: areisner@partners.org).

Equating the first and the last expressions, we have, in general,

$$H_1(z)\xi_1(n) = H_2(z)\xi_2(n) \quad (3)$$

for proper IIR systems $H_1(z)$ and $H_2(z)$, which does not include the input signal. This system ID technique is called the ‘‘blind’’ system ID because it does not involve the use of input signal for system ID.

Let $H_i(z) = N_i(z)D_i^{-1}(z)$ for $i = 1, 2$, where $D_i(z)$ is an n_i -th order monic polynomial in z and $N_i(z)$ is an m_i -th order polynomial in z , respectively. Then (3) is equivalent to

$$\begin{aligned} P_1(z)\xi_1(n) &= D_2(z)N_1(z)\xi_1(n) \\ &= D_1(z)N_2(z)\xi_2(n) = P_2(z)\xi_2(n) \end{aligned} \quad (4)$$

or alternatively in discrete-time domain,

$$[\xi_1(n+n_2+m_1)\cdots\xi_1(n) \quad -\xi_2(n+n_1+m_2)\cdots-\xi_2(n)]\mathbf{p} = 0, \quad (5)$$

where $\mathbf{p} \triangleq \begin{bmatrix} \mathbf{p}_1 \\ \mathbf{p}_2 \end{bmatrix}$ and \mathbf{p}_i , $i = 1, 2$, are vectors consisting of

the coefficients of $P_i(z)$. Given $G_i(z)$ and $P_i(z)$ for $i = 1, 2$, the 2-channel IIR systems considered in this paper are specified as follows:

Assumption 1: The class of 2-channel IIR systems considered in this paper satisfies the following assumptions C_1 and C_2 :

C_1 : Let $\boldsymbol{\theta} = \{\boldsymbol{\alpha}_1, \boldsymbol{\beta}_1, \boldsymbol{\alpha}_2, \boldsymbol{\beta}_2\}$, where $\boldsymbol{\alpha}_i$ and $\boldsymbol{\beta}_i$ are coefficients of the denominator and numerator polynomials in $G_i(z)$. Then there exists a predetermined constraint on $\boldsymbol{\theta}$ of the form:

$$F(\boldsymbol{\theta}) = F(\mathbf{p}) = F(\|\mathbf{p}\|\bar{\mathbf{p}}) = 0, \quad (6)$$

which yields unique non-trivial $\|\mathbf{p}\|$, where $\bar{\mathbf{p}} \triangleq \mathbf{p}/\|\mathbf{p}\|$.

C_2 : There exists a partition $\boldsymbol{\theta} = \boldsymbol{\theta}_1 \cup \boldsymbol{\theta}_2 \cup \cdots \cup \boldsymbol{\theta}_L$ such that

$$\mathbf{A}_i \boldsymbol{\theta}_i = \mathbf{b}_i, \quad i = 1, 2, \dots, L, \quad (7)$$

where $\mathbf{A}_i = \mathbf{A}_i(\mathbf{p}, \boldsymbol{\theta}_1, \dots, \boldsymbol{\theta}_{i-1})$, $\mathbf{b}_i = \mathbf{b}_i(\mathbf{p}, \boldsymbol{\theta}_1, \dots, \boldsymbol{\theta}_{i-1})$.

Now we present a blind system ID algorithm for this class of 2-channel IIR systems:

Blind Identification Algorithm: The class of 2-channel IIR systems satisfying C_1 and C_2 in Assumption 1 can be identified by the following procedure:

1) Formulate (5) into a matrix equation using the time series of ξ_1 and ξ_2 to form a set of over-constrained linear equations, i.e. $N > n_1 + m_1 + n_2 + m_2 + 2$:

$$\begin{bmatrix} \xi_1(n) & -\xi_2(n) \\ \vdots & \vdots \\ \xi_1(n-N) & \xi_2(n-N) \end{bmatrix} \mathbf{p} \triangleq [\boldsymbol{\Xi}_1 \quad -\boldsymbol{\Xi}_2] \mathbf{p} = 0, \quad (8a)$$

where N is the length of the time series used to solve (8a),

$$\xi_1(n) \triangleq [\xi_1(n+n_2+m_1)\cdots\xi_1(n)], \quad (8b)$$

and $\xi_2(n)$ is defined similarly from (5).

2) Identify $\bar{\mathbf{p}}$ from (8a) using singular value decomposition:

$$[\boldsymbol{\Xi}_1 \quad -\boldsymbol{\Xi}_2] = \mathbf{U}\boldsymbol{\Sigma}\mathbf{V}^T, \quad (9)$$

where the column of the unitary matrix \mathbf{V} corresponding to the minimum singular value is taken as the estimate of $\bar{\mathbf{p}}$.

3) Identify $\|\mathbf{p}\|$ from (6) and determine $\mathbf{p} = \|\mathbf{p}\|\bar{\mathbf{p}}$.

4) Identify $\boldsymbol{\theta}$ from (7) using \mathbf{p} .

Remark 1: Assumption 1 is the identifiability condition for $G_i(z)$, $i = 1, 2$. Firstly, although it is not possible to determine the length of \mathbf{p} from the homogeneous equation (5) alone, C_1 allows us to find $\|\mathbf{p}\|$ using the constraint equation (6) once $\bar{\mathbf{p}}$ is identified by solving (8a). In addition, C_2 enables us to pick out $G_i(z)$, $i = 1, 2$, from $P_i(z)$, $i = 1, 2$, by virtue of the mapping (7) between $\boldsymbol{\theta}$ and \mathbf{p} , although in general decomposition of $P_1(z)$ into $D_2(z)$ and $N_1(z)$ as well as that of $P_2(z)$ into $D_1(z)$ and $N_2(z)$ is not unique.

B. De-convolution Filter Design for Input Signal Recovery

Once the 2-channel IIR system is identified, the input signal may be recovered by inverting $G_1(z)$ or $G_2(z)$ if at least one of them has stable inverse. However, de-convolution filtering is required to recover the unknown input if both of the IIR systems have unstable zeros. In this paper we develop an algorithm to design a de-convolution filter that is applicable to multi-channel IIR systems using the notion of coprime transfer functions [8].

Lemma 1: Two stable, proper, real-rational transfer functions $M_1(z)$ and $M_2(z)$ are coprime if they have no common zeros outside the unit circle and at least one of them has zero relative degree. If $M_1(z)$ and $M_2(z)$ are coprime, there exist stable, proper, real rational transfer functions $W_1(z)$ and $W_2(z)$ satisfying the Bezout identity:

$$M_1(z)W_1(z) + M_2(z)W_2(z) = 1. \quad (10)$$

De-convolution Algorithm: The unknown input signal $u(n)$ can always be recovered from the output signal measurements $y_i(n)$, $i = 1, 2$ using the identified IIR system coefficients $\boldsymbol{\theta}$:

$$u(n) = \frac{\eta_1(z)}{\alpha_2(z, \boldsymbol{\theta})} (z - z_0)^{r_1} y_1(n) + \frac{\eta_2(z)}{\alpha_1(z, \boldsymbol{\theta})} y_2(n), \quad (11)$$

where $|z_0| < 1$, $G_2(z_0, \boldsymbol{\theta}) \neq 0$, r_1 is the relative degree of $G_1(z, \boldsymbol{\theta})$, and $\eta_1(z)$ and $\eta_2(z)$ are polynomials in z of order n_2 and $(n_1 - 1)$, respectively, satisfying

$$(z - z_0)^{r_1} \beta_1(z, \boldsymbol{\theta}) \eta_1(z) + \beta_2(z, \boldsymbol{\theta}) \eta_2(z) = \alpha_1(z, \boldsymbol{\theta}) \alpha_2(z, \boldsymbol{\theta}). \quad (12)$$

Outline of Proof: From (1) $(z - z_0)^{r_1} G_1(z, \boldsymbol{\theta})$ is an IIR system with zero relative degree, and thus $(z - z_0)^{r_1} G_1(z, \boldsymbol{\theta})$ and $G_2(z, \boldsymbol{\theta})$ are coprime. Hence, by the above lemma, there exist stable proper IIR systems $W_1(z)$ and $W_2(z)$ satisfying

$$(z-z_0)^{n_1} G_1(z, \boldsymbol{\theta}) W_1(z) + G_2(z, \boldsymbol{\theta}) W_2(z) = 1. \quad (13)$$

Constructing $W_1(z, \boldsymbol{\theta})$ and $W_2(z, \boldsymbol{\theta})$ as

$$W_1(z, \boldsymbol{\theta}) = \eta_1(z) \alpha_2^{-1}(z, \boldsymbol{\theta}), \quad W_2(z, \boldsymbol{\theta}) = \eta_2(z) \alpha_1^{-1}(z, \boldsymbol{\theta}). \quad (14)$$

Then (13) reduces to the polynomial identity (12). Multiplying $u(n)$ to both sides of (13) yields (11).

Since $\eta_1(z)$ and $\eta_2(z)$ together give $n_1 + n_2 + 1$ unknowns and both sides of (12) are polynomials of order $n_1 + n_2$, (12) results in a set of $n_1 + n_2 + 1$ linear equations with $n_1 + n_2 + 1$ unknowns, $\mathbf{A}\boldsymbol{\eta} = \bar{\mathbf{a}}$ (see Fig. 1), where

$$(z-z_0)^{n_1} \beta_1(z, \boldsymbol{\theta}) = \bar{\beta}_{n_1}^{(1)} z^{n_1} + \dots + \bar{\beta}_0^{(1)} \quad (15)$$

$$\alpha_1(z, \boldsymbol{\theta}) \alpha_2(z, \boldsymbol{\theta}) = \bar{\alpha}_{n_1+n_2} z^{n_1+n_2} + \dots + \bar{\alpha}_0$$

The matrix \mathbf{A} should be nonsingular for the existence of $\boldsymbol{\eta}$, the coefficients of the de-convolution filter. First, it is evident from the structure of \mathbf{A} that the columns of the sub-matrix \mathbf{A}_2 are linearly independent of the columns of the sub-matrices \mathbf{A}_1 and \mathbf{A}_3 as well as of each other because $\bar{\beta}_{n_1}^{(1)} \neq 0$. It then follows that for non-singularity of \mathbf{A} the sub-matrix $[\mathbf{A}_1 \quad \mathbf{A}_3]$ should be nonsingular. Noting that $[\mathbf{A}_1 \quad \mathbf{A}_3]$ is the Sylvester matrix of $(z-z_0)^{n_1} \beta_1(z, \boldsymbol{\theta})$ and $\beta_2(z, \boldsymbol{\theta})$, these polynomials should be coprime, which is always guaranteed because $G_1(z, \boldsymbol{\theta})$ and $G_2(z, \boldsymbol{\theta})$ have no common poles and zeros and z_0 is chosen such that $G_2(z_0, \boldsymbol{\theta}) \neq 0$. Therefore, $u(n)$ can always be recovered using (11). Q.E.D. \square

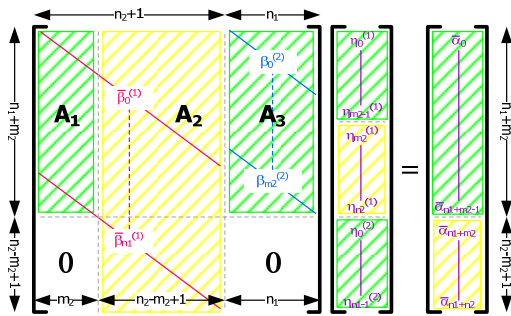


Fig. 1. Matrix equation for the design of de-convolution filter.

C. Persistent Excitation and Model Identifiability Analysis

Let $P_1(z) = p_{n_2+m_1}^{(1)} z^{n_2+m_1} + \dots + p_0^{(1)}$ and rewrite (5) as:

$$\xi_1(n+n_2+m_1) = \mathbf{q}^T \boldsymbol{\Phi}(n), \quad (16)$$

where $\mathbf{q} \triangleq [p_{n_2+m_1}^{(1)}]^{-1} [p_{n_2+m_1-1}^{(1)} \dots p_0^{(1)} \quad \mathbf{p}_2^T]^T$, and

$$\boldsymbol{\Phi}(n) = [-\xi_1(n+n_2+m_1-1) \dots -\xi_1(n) \quad \xi_2(n)]^T. \quad (17)$$

Given a time series of ξ_1 and ξ_2 , (16) can be formulated into:

$$\begin{bmatrix} \xi_1(n+n_2+m_1) \\ \vdots \\ \xi_1(n+n_2+m_1-N) \end{bmatrix} = \begin{bmatrix} \boldsymbol{\Phi}^T(n) \\ \vdots \\ \boldsymbol{\Phi}^T(n-N) \end{bmatrix} \mathbf{q} \triangleq \boldsymbol{\Phi} \mathbf{q}. \quad (18)$$

where $N > n_1 + m_1 + n_2 + m_2 + 2$. It can be solved for \mathbf{q} using the least-squares method if $\boldsymbol{\Phi}^T \boldsymbol{\Phi}$ is nonsingular, which means that ξ_1 and ξ_2 persistently excites the system so that \mathbf{p} is determined to scale. Therefore, the PE condition is given by the positive definiteness of $\boldsymbol{\Phi}^T \boldsymbol{\Phi}$:

$$\frac{1}{N+1} \sum_{k=n-N}^n \boldsymbol{\Phi}(k) \boldsymbol{\Phi}^T(k) = \frac{1}{N+1} \boldsymbol{\Phi}^T \boldsymbol{\Phi} > \mathbf{0}. \quad (19)$$

Once the PE condition is satisfied, the MI condition becomes trivial: the model structure (16) is always identifiable, since it is a moving-average model [9].

D. Asymptotic Variance Analysis

In 2-channel blind IIR system ID, the model coefficients are determined by minimizing the error associated with (3):

$$\varepsilon(n, \hat{\boldsymbol{\theta}}) \triangleq H_1(z, \hat{\boldsymbol{\theta}}) \xi_1(n) - H_2(z, \hat{\boldsymbol{\theta}}) \xi_2(n), \quad (20)$$

which is defined as the empirical measurement error. Following [9] it can be shown that the variance of $\varepsilon(n)$ in estimating $\boldsymbol{\theta}$ asymptotically converges to

$$\begin{aligned} \text{var}(\hat{\boldsymbol{\theta}} - \boldsymbol{\theta}_0) &\cong \frac{1}{N} \lambda_N(\boldsymbol{\theta}_0) \mathbf{S}_N(\boldsymbol{\theta}_0) \\ &\triangleq \frac{1}{N} \lambda_N(\boldsymbol{\theta}_0) \left[\frac{1}{N} \sum_{n=1}^N \boldsymbol{\Psi}(n, \boldsymbol{\theta}_0) \boldsymbol{\Psi}^T(n, \boldsymbol{\theta}_0) \right]^{-1}, \end{aligned} \quad (21)$$

where $\lambda_N(\boldsymbol{\theta}) \triangleq \frac{1}{N} \sum_{n=1}^N \varepsilon^2(n, \boldsymbol{\theta})$ is the empirical measurement

error variance, $\boldsymbol{\Psi}(n, \boldsymbol{\theta}) \triangleq \frac{d\varepsilon(n, \boldsymbol{\theta})}{d\boldsymbol{\theta}}$ is the sensitivity of $\varepsilon(n, \boldsymbol{\theta})$ to $\boldsymbol{\theta}$, and $\mathbf{S}_N(\boldsymbol{\theta})$ is the inverse of the sensitivity covariance matrix. The variance is not computable since it is evaluated at $\boldsymbol{\theta}_0$. However, the following empirical approximation using the estimate $\hat{\boldsymbol{\theta}}$ suffices in many applications:

$$\text{var}(\hat{\boldsymbol{\theta}} - \boldsymbol{\theta}_0) \cong \frac{1}{N} \lambda_N(\hat{\boldsymbol{\theta}}) \mathbf{S}_N(\hat{\boldsymbol{\theta}}), \quad (22)$$

The variance $\text{var}(G_i(z, \hat{\boldsymbol{\theta}}) - G_i(z, \boldsymbol{\theta}_0))$, $i=1,2$, of estimating $G_1(z)$ and $G_2(z)$ can then be obtained as follows [9]:

$$\text{var}(G_i(z, \hat{\boldsymbol{\theta}}) - G_i(z, \boldsymbol{\theta}_0)) \cong \frac{dG_i^T(z, \hat{\boldsymbol{\theta}})}{d\boldsymbol{\theta}} \text{var}(\hat{\boldsymbol{\theta}} - \boldsymbol{\theta}_0) \frac{dG_i(z^{-1}, \hat{\boldsymbol{\theta}})}{d\boldsymbol{\theta}}. \quad (23)$$

III. METHODS

A. Gray-Box Model of 2-Channel Cardiovascular System

The blind IIR system ID algorithm developed in this paper is applicable to a class of CV system models. The ‘‘asym-

metric T-tube” model [11], which meets the basic assumptions, C_1 and C_2 , of the algorithm, is used as an exemplary case study. It is noted, however, that the algorithm may be extended to more complex representations of the CV system, possibly with additional CV signal measurements as well as increased computational cost.

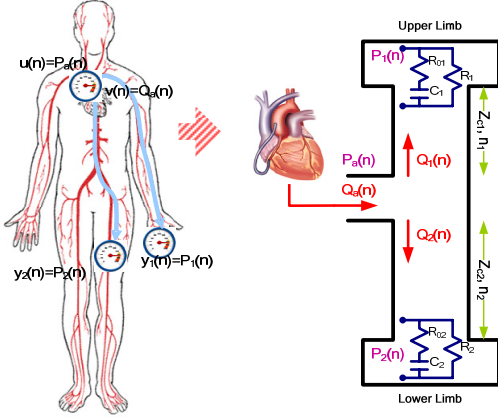


Fig. 2. Asymmetric T-tube model of a 2-channel CV system.

The “asymmetric T-tube” model represents the CV system by a parallel connection of two distinct transmission lines (TL’s) with associated terminal load impedances (see Fig. 2). The TL’s describe the proximal vessels, whereas the load impedances represent the resultant effect of the distal circulation, i.e. the small extremity vessels. In Fig. 2, $P_a(n)$, $P_1(n)$, $P_2(n)$ and $Q_a(n)$, $Q_1(n)$, $Q_2(n)$ are the BP and BF signals at the aortic, upper-limb and lower-limb locations. Note that the subscripts 1 and 2 represent the upper-limb and lower-limb quantities. The parameters n_1 and n_2 are the time delays (in number of samples) associated with the BP and BF wave propagation from aortic to peripheral locations, Z_{c1} and Z_{c2} are the characteristic impedances, C_1 and C_2 are the terminal compliances, R_1 and R_2 are the terminal resistances, and R_{01} and R_{02} are the high-frequency matching resistances [11].

The transfer function from $P_a(n)$ to $P_i(n)$ becomes:

$$G_i(z, \Theta) \triangleq \frac{\beta_i(z, \Theta)}{\alpha_i(z, \Theta)} = \frac{z^{n_i+1} + [(a_i + b_i)/F_s - 1]z^{n_i}}{z^{2n_i+1} + (a_i/F_s - 1)z^{n_i} + b_i/F_s}, \quad (24)$$

where $\Theta \triangleq \{n_1, n_2, \theta\}$, $\theta \triangleq \{a_1, a_2, b_1, b_2\}$, and

$$a_i \triangleq \frac{2R_{0i} + R_i}{2R_{0i}C_i(R_{0i} + R_i)}, \quad b_i \triangleq \frac{R_i}{2R_{0i}C_i(R_{0i} + R_i)}. \quad (25)$$

The parallel arrangement of the TL’s in the asymmetric T-tube model suggests that the root impedance at the aorta is given by $Z_a(z, \Theta) = Z_1(z, \Theta) // Z_2(z, \Theta)$:

$$Z_i(z, \Theta) \triangleq Z_{ci} \left[1 + \Gamma_i(z, \Theta) z^{2n_i} \right] / \left[1 - \Gamma_i(z, \Theta) z^{-2n_i} \right]. \quad (26)$$

where $Z_{ci} \triangleq \frac{P_i^+}{Q_i^+} = \frac{R_{0i}R_i}{R_{0i} + R_i}$ [11]. Then $Z_a(z, \Theta)$ becomes:

$$Z_a(z, \Theta) \triangleq \frac{Z_{c1}Z_{c2}\alpha_1(z, \Theta)\alpha_2(z, \Theta)}{Z_{c1}\alpha_1(z, \Theta)\tilde{\alpha}_2(z, \Theta) + Z_{c2}\tilde{\alpha}_1(z, \Theta)\alpha_2(z, \Theta)}, \quad (27)$$

where $\tilde{\alpha}_i(z, \Theta) \triangleq z^{2n_i+1} + (a_i/F_s - 1)z^{n_i} - b_i/F_s$, $i = 1, 2$.

Remark 2: It is easy to prove that the transfer functions $G_i(z)$, $i = 1, 2$, are indeed identifiable. Considering $P_2(z)$,

$$P_2(z) \triangleq \alpha_1(z)\beta_2(z) = z^{2n_1+2} + p_{2n_1+1}^{(2)}z^{2n_1+1} + p_{2n_1}^{(2)}z^{2n_1} + p_1^{(2)}z + p_0^{(2)}, \quad (28)$$

where $p_{2n_1+2}^{(2)} = 1$ since $\beta_2(z)$ is monic, which satisfies C_1 .

In addition, a_1 and b_1 are uniquely determined from \mathbf{p}_2 :

$$a_1 = F_s \left[\frac{p_{2n_1}^{(2)}p_1^{(2)}}{p_0^{(2)}} + 1 \right], \quad b_1 = F_s p_1^{(2)}. \quad (29)$$

Using $P_1(z) \triangleq \alpha_2(z)\beta_1(z)$, we obtain $p_{2n_1+2}^{(2)} = 1$, and a_2 and b_2 are uniquely determined from \mathbf{p}_1 , which, together with (29), means that C_2 is also satisfied. Therefore, $G_i(z)$, $i = 1, 2$, are identifiable.

B. Experimental Protocol

Under the experimental protocol #01-055 approved by the Massachusetts Institute of Technology Committee of Animal Care, invasive CV BP and BF signals were collected from an anesthetized pig, details of which can be found in [6].

C. System Identification and Aortic Signal Recovery

From the experimental data obtained from the pig, totally 83 segments of data, each having 2,000 samples of aortic BP and BF as well as radial and femoral BP, were collected. In order to apply the blind system ID algorithm developed in this paper to these data, the following challenges specific to (24) and (27) had to be taken care of:

1) The blind system ID is applicable only to the ID of distinct channel dynamics [5], although the CV system model has $Z_a(z, \Theta)$ as common dynamics. Therefore, we identified the CV system model in two steps: first we used our blind system ID algorithm to identify (24) using $y_1(n)$ and $y_2(n)$, after which we used Θ to identify (27).

2) In the absence of aortic measurements, the time delays n_1 and n_2 , which determine the orders of (24), are unknown prior to ID. Using the peripheral BP measurements, however, the “differential” time delay, $\Delta n \triangleq n_2 - n_1$, can be measured as the end-diastolic or foot-to-foot interval between the peripheral BP signals. This Δn plays a crucial role in accurately identifying $G_i(z)$, $i = 1, 2$, by imposing a restriction on their orders. We iteratively applied our blind system ID algorithm to (24) and optimized the solution over a range of physiologically relevant values of n_1 , with n_2 restricted to $n_2 = n_1 + \Delta n$.

3) By virtue of the physical implications of the coefficients in the asymmetric T-tube model, Θ parameterizing (24) can

be constrained as follows:

$$\Theta \in \mathbf{D}_\Theta = \{\Theta | n_i > 0, a_i > 0, b_i > 0, a_i > b_i, i=1,2\}, \quad (30)$$

which, together with the use of Δn mentioned above, results in the constrained least-squares formulation (31):

$$\Theta = \min_{\Theta \in \mathbf{D}_\Theta} \left[\min_{n_i \in \mathbf{D}_\Theta} \|G_1^{-1}(z, \Theta)y_1(n) - G_2^{-1}(z, \Theta)y_2(n)\|_2 \right]. \quad (31)$$

4) It is evident from (25) that the asymmetric T-tube model, which has n_i , C_i , R_i and R_{0i} , $i=1,2$, as unknowns, cannot be uniquely characterized by Θ , which yields only six coefficients pertaining to $G_i(z)$, $i=1,2$ in (24). Noting from (27) that $Z_a(z, \Theta)$ cannot be determined directly from Θ , additional constraints need to be augmented to Θ . The incompetence to determine the scale of $Z_a(z, \Theta)$ is inherent due to the absence of any BF measurements. However, the shape of $Z_a(z, \Theta)$ can be determined by utilizing the constraint that its denominator should have the Windkessel pole as its root. To identify the shape of $Z_a(z, \Theta)$, therefore, this paper estimated the Windkessel pole using the two peripheral BP signals and augmented the following constraint to Θ , which allows us to determine the relative scales of C_i , R_i and R_{0i} , $i=1,2$:

$$Z_{c1}\alpha_1(\lambda_w, \Theta)\alpha_2(\lambda_w, \Theta) + Z_{c2}\alpha_1(\lambda_w, \Theta)\alpha_2(\lambda_w, \Theta) = 0, \quad (32)$$

where λ_w is the Windkessel pole.

Once $G_1(z)$, $G_2(z)$ and $Z_a(z)$ were identified, the aortic BP and BF signals were recovered using their inverses:

$$\begin{aligned} \hat{u}(n) &= G_1^{-1}(z, \Theta)y_1(n) + G_2^{-1}(z, \Theta)y_2(n) \\ \hat{v}(n) &= Z_a^{-1}(z, \Theta)\hat{u}(n) \end{aligned} \quad (33)$$

To guarantee the identifiability of the CV dynamics (24) and (27), the richness of the data was evaluated by examining the PE condition (19) for each data segment. Furthermore, to assess the level of confidence on the identified CV dynamics, the asymptotic variance of Θ and the resulting $G_i(z)$, $i=1,2$ was evaluated by (22) and (23).

IV. RESULTS AND DISCUSSION

The experimental results suggest that the algorithm developed in this paper is able to identify the CV dynamics with fidelity and reliability, over wide-ranging physiologic conditions. Fig. 3 shows a typical result of CV dynamics ID and aortic signal recovery, where the upper two plots show the true and identified frequency responses of $G_1(z)$ and $G_2(z)$, and the lower two plots show the true and recovered aortic BP and BF signals. Using two distinct peripheral BP signals (i.e. radial and femoral in this paper), our algorithm could provide high-fidelity estimates of the CV dynamics as well as accurately recover the aortic BP and BF signals for all the 83 segments of data.

To further quantify the performance of the proposed algorithm, an averaged transfer function representing nominal

upper-limb CV dynamics [1] was used as a benchmark performance. The proposed and the averaged methods were compared using the aortic BP recovery error, $\|u(n) - \hat{u}(n)\|_2$, and the accuracy of the clinical features (e.g. ejection duration and systolic BP) extracted from the recovered aortic BP signals over the 83 experimental data segments. Table I summarizes the results with bias the standard deviation (STD) as evaluation metrics, which clearly suggests that the proposed method far outperforms the averaged method: on the average, the aortic BP recovery was improved by 40%; besides, the estimation of ejection duration and systolic BP was also improved, particularly in terms of the STD (50% for the ejection duration and 71% for the systolic BP). This significant benefit of the proposed method suggests that the wide-ranging physiologic conditions of the CV system cannot be described by a single predetermined transfer function that is widely used in practice [1].

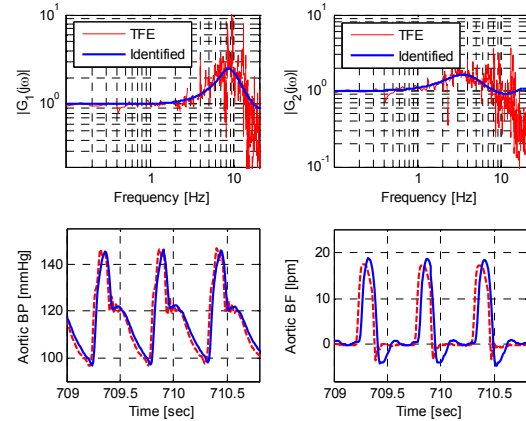


Fig. 3. Identified frequency responses and recovered aortic BP and BF signals at $t=710s$. Dashed and solid lines are true and identified/recovered quantities, respectively. True and predicted CO: 3.8lpm and 3.9lpm.

The examination of the PE condition (19) for the 83 segments of the radial and femoral BP data showed that the PE condition was met for all the 83 segments of data. The PE analysis also revealed that the well-posedness of the CV dynamics ID (31) is closely related to the heart rate (HR) frequency, F_{HR} (which represents the characteristics of the excitation signal), and the frequency F_{G_2} at which $|G_2(j\omega)|$ attains its maximum (which represents the physiologic condition): the smaller $|F_{HR} - F_{G_2}|$, the better the condition number of $\Phi^T \Phi$. This finding can be interpreted as follows: considering that the most important feature of the frequency responses $G_i(j\omega)$, $i=1,2$, to be identified with accuracy is the location F_{G_i} and the magnitude $|G_i(2\pi F_{G_i} j)|$ of their peaks, the quality of identifying the CV system hinges upon how well the frequency range around F_{G_2} is excited by the aortic BP (or, equivalently BF) signal. This suggests that care

must be taken when we interpret the identified CV dynamics associated with large $|F_{HR} - F_{G_2}|$.

TABLE I. PERFORMANCE OF PROPOSED AND AVERAGED METHODS

	Proposed Method	Averaged Method
$\ u(n) - \hat{u}(n)\ _2$	2.7 +/- 0.8mmHg	4.5 +/- 2.8mmHg
Ejection Duration (0.21 +/- 0.07s)	0 +/- 0.01s (R ² =0.9109)	0 +/- 0.02s (R ² =0.7665)
Systolic BP (124 +/- 76mmHg)	2.3 +/- 2.3mmHg (R ² =0.9925)	3.1 +/- 7.9mmHg (R ² =0.9309)

TABLE II. RESULTS OF ASYMPTOTIC VARIANCE ANALYSIS, N=250~2,000

	N=250	N=500	N=1,000	N=2,000
$\sqrt{\lambda_N(\hat{\Theta})}$	1.92 (2.31%)	1.91 (2.30%)	1.88 (2.26%)	1.87 (2.24%)
$\ S_N(\hat{\Theta})\ $	3262	2853	3189	3001
var $[\delta n_1]$	0.019 (0.29%)	0.009 (0.12%)	0.005 (0.07%)	0.002 (0.03%)
var $[\delta a_1]$	94.12 (4.68%)	36.64 (2.07%)	24.19 (1.12%)	10.88 (0.52%)
var $[\delta b_1]$	21.23 (0.39%)	7.880 (0.17%)	4.303 (0.09%)	2.225 (0.04%)
var $[\delta n_2]$	0.019 (0.08%)	0.009 (0.04%)	0.005 (0.02%)	0.002 (0.01%)
var $[\delta a_2]$	0.801 (1.11%)	0.373 (0.46%)	0.197 (0.28%)	0.093 (0.13%)
var $[\delta b_2]$	0.158 (0.34%)	0.073 (0.15%)	0.033 (0.08%)	0.016 (0.04%)

The results of asymptotic variance analysis give more insights into the reliability of the system ID. First, Table II summarizes the results of the asymptotic variance analysis for the data length of 250, 500, 1,000 and 2,000, which show that the asymptotic variance of Θ decreases approximately in proportion to N , as predicted by the analysis. Therefore, the reliability of parameter estimation can be improved by increasing the length of the data used for system ID. Table II also shows that n_2 and a_1 has the smallest and the largest asymptotic variance, respectively, which accords with our eigenstructure analysis of S_N : the eigenvector associated with the smallest and the largest eigenvalues were mostly aligned with the directions of n_2 and a_1 , meaning that $\varepsilon(n)$ is the most and the least sensitive to n_2 and a_1 , respectively. Hence, those elements of Θ having large sensitivity on the empirical measurement error are relatively easier to identify than their small-sensitivity counterparts.

Quantifying λ_N over the 83 segments of data showed that its values were limited within 4% of the associated mean BP values, with the average of 2.3% (see Table II), suggesting that the asymmetric T-tube model is an efficient representation of the CV system considered in this paper.

V. CONCLUSION

Identifying the CV dynamics from limited peripheral BP observation is a challenging problem. This paper has devel-

oped an effective blind system identification algorithm for characterizing the CV dynamics, a de-convolution algorithm for stable inversion, and analysis and design tools for evaluating the richness of observed signals, the estimation error variance and the parameter sensitivity. The utility and potential applications of this identification method abound, but many of them are yet to be explored.

REFERENCES

- [1] S. Hope, D. Tay, I. Meredith, and J. Cameron, "Use of arterial transfer functions for the derivation of aortic waveform characteristics," *Journal of Hypertension*, vol. 21, no. 7, pp. 1299-1305, July 2003.
- [2] J. Jansen, J. Schreuder, J. Mulier, N. Smith, J. Settels, and K. Wesseling, "A comparison of cardiac output derived from the arterial blood pressure wave against thermodilution in cardiac surgery patients," *British Journal of Anaesthesia*, vol. 87, no. 2, pp. 212-222, August 2001.
- [3] C. Quick, D. Berger, R. Stewart, G. Laine, C. Hartley, and A. Noordergraaf, "Resolving the hemodynamic inverse problem," *IEEE Transactions on Biomedical Engineering*, vol. 53, no. 3, pp. 361-368, March 2006.
- [4] W. Stok, B. Westerhof, and J. Karemaker, "Changes in finger-aorta pressure transfer function during and after exercise," *Journal of Applied Physiology*, vol. 101, no. 4, pp. 1207-1214, October 2006.
- [5] Y. Zhang and H. Asada, "Blind system identification of noncoprime multichannel systems and its application to noninvasive cardiovascular monitoring," *ASME Journal of Dynamic Systems, Measurement and Control*, vol. 126, no. 4, pp. 834-847, December 2004.
- [6] D. McCombie, A. Reisner, and H. Asada, "Laguerre model blind system identification: cardiovascular dynamics estimated from multiple peripheral circulatory signals," *IEEE Transactions on Biomedical Engineering*, vol. 52, no. 11, pp. 1889-1901, November 2005.
- [7] M. Gurelli and C. Nikias, "EVAM: An eigenvector-based algorithm for multichannel blind deconvolution of input colored signals," *IEEE Transactions on Signal Processing*, vol. 43, no. 1, pp. 134-149, January 1995.
- [8] J. Doyle, B. Francis, A. Tannenbaum, *Feedback Control Theory*. New York, NY: Macmillan Publishing, 1992.
- [9] L. Ljung, *System Identification Theory for the User*. Upper Saddle River, NJ: Prentice-Hall, 1999.
- [10] W. Nichols and M. O'Rourke, *McDonald's blood flow in arteries*. London, United Kingdom: Arnold, 1998.
- [11] K. Campbell, R. Burattini, D. Bell, R. Kirkpatrick, and G. Knowlton, "Time-domain formulation of asymmetric T-tube model of arterial system," *American Journal of Physiology*, vol. 258, pp. 1761-1774, 1990.
- [12] J. Kong, *Electromagnetic wave theory*. Cambridge, MA: EMW Publishing, 2000.